Food Chemistry 431 (2024) 137160

Contents lists available at ScienceDirect

Food Chemistry

journal homepage: www.elsevier.com/locate/foodchem

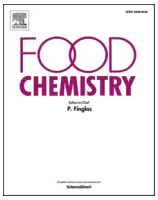

Flaxseed oleosomes: Responsiveness to physicochemical stresses, tribological shear and storage

Hasan H. Kara [a,b], Andrea Araiza-Calahorra [a], Neil M. Rigby [a], Anwesha Sarkar [a,*]

[a] Food Colloids and Bioprocessing Group, School of Food Science and Nutrition, University of Leeds, Leeds LS2 9JT, UK
[b] Nutrition and Dietetics Department, Faculty of Health Sciences, Necmettin Erbakan University, 42090 Meram, Konya, Turkiye

ARTICLE INFO

Keywords:
Oil bodies
Microstructure
Friction
Electrophoresis
Viscosity
Tribology

ABSTRACT

This study aimed to extract oleosomes (OLs) from flaxseeds and assess their response to environmental conditions during storage (pH and ionic strengths), shear and tribological stresses. Our hypothesis was that a shear-induced instability will enable OLs to exhibit favourable lubrication performance. During storage, OLs exhibited resistance to droplet aggregation for up to 6 weeks owing to the proteins (3.5–152.8 kDa molecular weights) stabilizing the OL droplets. However, presence of divalent (Ca^{2+}) ions induced destabilization with marked increase in droplet size ($p < 0.05$). OLs demonstrated shear thinning behaviour, displaying an order of magnitude higher viscosity than flaxseed oil (FSO) at low shear rates (<10 s^{-1}). Strikingly, OLs mirrored the frictional profile of FSO regardless of entrainment speeds, due to droplet coalescence, validating the hypothesis. Such kinetic stability with shear-induced coalescing feature of OLs hold strong potential for future plant-based food development, particularly in achieving desired mouthfeel characteristics.

1. Introduction

Oleosomes, also known as oil bodies, are micron-sized, micelle-like organelles found in the nature that serve as intracellular lipid storage structures. They possess a distinctive composition, consisting of a hydrophobic triglyceride core surrounded by phospholipids and various embedded alkaline proteins, including oleosins, caleosins, and steroleocins (Acevedo-Fani, Dave, & Singh, 2020; Chang et al., 2013; De Chirico, di Bari, Foster, & Gray, 2018). Previous research has primarily focused on investigating oleosomes in traditional oilseed crops such as sunflower, soybean, and rapeseed (Nikiforidis, Kiosseoglou, & Scholten, 2013; Qi et al., 2017; Romero-Guzmán, 2020). Typically, oleosomes isolated from oilseeds contain approximately 94 – 98% neutral lipid, 0.6 – 2% phospholipid, and 0.6% protein. However, the specific lipid composition can vary across different plant species (Payne, Lad, Foster, Khosla, & Gray, 2014). These inherently assembled structures of oleosomes found in oilseeds possess a highly complex interfacial configuration. This unique configuration plays a crucial role in protecting the polyunsaturated triglycerides (*i.e.*, the oil) naturally encapsulated within the oleosomes from adverse environmental influences (Nikiforidis, 2019).

Flaxseed (*Linum usitatissimum* L.) is an important plant source of health-promoting compounds such as α-linolenic acid, good quality protein, and phytochemicals such as flavonoids, lignans and phenolic acids (Kajla, Sharma, & Sood, 2015; Oomah, 2001). Flaxseed oil is known for its high content of the omega-3 fatty acid called linolenic acid, which accounts for approximately 55% of the oil (Oomah, 2001). Interestingly, the flaxseed oleosomes exhibit a protective effect on the naturally encapsulated flaxseed oil, preventing auto-oxidation. This unique attribute makes flaxseed oleosomes an intriguing member of the oleosome family and an attractive candidate for investigation. However, unlike many well-studied oleaginous seeds (*e.g.* rapeseed, soybean, sunflower), flaxseeds have significant amounts of mucilaginous polysaccharide making the extraction process challenging (Chen, Xu, & Wang, 2006). Furthermore, up until now, there has been a lack of comprehensive studies that have systematically characterized flaxseed oleosomes (OLs). Such investigations would significantly enhance our understanding of how OLs are able to provide remarkable stability against oxidation, despite containing a substantial amount of unsaturated fatty acids. Therefore, characterizing the composition and proteins in flaxseed oleosomes, as well as their microstructural behaviour over storage may help define key design rules that may inspire the design of future biomimetic oleosomes containing long-chain unsaturated fatty acids.

* Corresponding author.
E-mail address: A.Sarkar@leeds.ac.uk (A. Sarkar).

https://doi.org/10.1016/j.foodchem.2023.137160
Received 16 June 2023; Received in revised form 4 August 2023; Accepted 13 August 2023
Available online 14 August 2023

In fact, environmental stresses such as pH and ionic strengths have varying degree of destabilization effects on oleosome characteristics obtained from different sources. In rapeseed oleosome, significant coalescence of droplets were found at pH 7.0 in presence of divalent cations (Ca^{2+}, Mg^{2+}) unlike monovalent ions (Na^{+}, K^{+}) (Romero-Guzmán et al., 2020b), largely attributed to charged species of proteins and phospholipids at the interface of oleosome droplets driving electrostatic interactions and consequently kinetic stability in oleosomes (Nikiforidis & Kiosseoglou, 2011). In soybean oleosomes, the particle size and surface hydrophobicity of oleosome-associated proteins were found to be significantly influenced by pH levels. Alkaline pH treatments (pH 8.0 – 11.0) were found to induce an increase in the β-sheets conformation of oleosome-associated proteins contributing to soybean oleosome aggregation (Qi et al., 2017). However, to our knowledge there has been no systematic study that has evaluated the stability of flaxseed oleosomes as a function of pH and ionic strengths (mono and divalent ions) over time, which will be tackled in this study.

Rheological properties of oleosomes are important on their own and also when they are added to other products. For example, in the case of soybean oleosome emulsions, they exhibit weak gel-like behavior, with viscosity increasing as the oil content increases, and showing instability under certain environmental conditions (Wu et al., 2012). Given the observed instability of oleosomes, it is important to understand the implication of droplet breakup under high shear conditions. We hypothesize that a shear-induced instability in oleosome will enable them to exhibit favourable lubrication behaviour. To date, there have been very few tribological studies *i.e.* studies measuring friction and lubrication of oleosomes when they are incorporated within colloidal systems, such as emulsion gels (Yang et al., 2020). This suggests a significant gap in our understanding of the tribology of oleosomes themselves. One may question, how do oleosomes lubricate surfaces? – Is it primarily through shear-induced coalescence, or does the viscosity of the oleosomes play a key role in such lubrication phenomena?

This study thus aimed to characterize the physicochemical and microstructural properties of flaxseed oleosome as a function of environmental stresses (pH, ionic strengths), storage time as well as shear in the rheological and tribological limits. In the study, oleosomes were obtained from flaxseed by aqueous-based green extraction method subjected to different pHs (pH 1.0 – 7.0), ionic strengths (0–200 mM NaCl, 0–50 mM $CaCl_2$) and tribological conditions, and characterized using a suite of techniques such as sodium dodecyl sulphate polyacrylamide gel electrophoresis (SDS-PAGE), zeta-potential, static light scattering, microscopy across length scales, rheology and tribology. Findings from this fundamental study will provide important insights about the structure and properties of flaxseed oleosomes, which can be used as a promising alternative in the formation of natural plant-based emulsions for developing plant-based foods as well as carriers for various bioactive components.

2. Materials and methods

2.1. Materials

Flaxseeds were obtained from a local supermarket (Migros, Konya) in Turkey. Smooth elastomeric (polydimethylsiloxane (PDMS, Sylgard 184, Dow Corning, Midland, MI, USA) tribopairs *i.e.* PDMS ball (∅ 47 mm) and disc (∅ 19 mm – 4 mm thickness) with surface roughness of nearly 50 nm were purchased from PCS instruments, London, UK. The sodium dodecyl sulphate polyacrylamide gel electrophoresis (SDS-PAGE) chemicals were purchased from Invitrogen Ltd. (Paisley, UK). All other chemicals used in this study were of analytical grade and were purchased from Signa Aldrich, Dorset, UK unless otherwise specified. All dispersions were prepared with Milli-Q water having a resistivity of 18.2 MΩ.cm at 25 °C (Milli-Q apparatus, Millipore, Bedford, MA, USA).

2.2. Methods

2.2.1. Extraction of oleosomes

Oleosome extraction from flaxseeds was carried out as shown in Fig. 1 using previously described aqueous extraction routes (Chen & Ono, 2010). Briefly, flaxseeds were milled using a coffee grinder (Krups F203, Solingen, Germany) and mixed with MilliQ water (1:10 v/v) and kept at 4 °C for 72 h to allow hydration. In grinding, care was taken to ensure that the particle size was large enough not to pass through a 1 mm mesh sieve and small enough to pass through a 1.6 mm mesh sieve. After the hydration stage, the milled flaxseed suspension was homogenized with a kitchen blender (XJ-10402, Argos, Milton Keynes, UK) at speed position 2 for 1 min. Then the dispersion was collected in 50 mL centrifuge tubes and centrifuged at 4,612 *g* for 15 min at 4 °C (Rotina 380 R, Hettich, Germany) to separate the flaxseed milk containing the oleosomes from the solid residues. After this, the flaxseed milk was further centrifuged in an ultra-high-speed centrifuge (Avanti J-301, Beckman Coulter, Brea, California, USA) at 75,600 *g* for 20 min at 4 °C, and the oleosome (cream) layer (OL) *i.e.* the supernatant was collected from the top. The same centrifugation process was repeated three times to increase the level of purification. The entire process of extraction was carried out at 4 °C and the obtained OL was stored under refrigerated conditions (4 °C) for further analysis by adding 0.02 wt% sodium azide.

2.2.2. Effects of pH and ionic strengths

To understand the effect of pH on stability of OL, 0.01 N HCl or 0.01 N NaOH was used to decrease the pH levels ranging from pH 1.0 – 7.0. In addition, to understand the influence of ionic strengths, OL samples were tested for their stability after addition of 50 or 200 mM NaCl, 5 or 50 mM $CaCl_2$ as well as a combination of mono- and divalent cations (200 mM NaCl + 50 mM $CaCl_2$). The original OL sample extracted at pH 5.4, as well as the samples subjected to different pHs and ionic strengths were subjected to storage stability study for 9 weeks at 4 °C.

2.2.3. Proximate composition

The proximate composition of the extracted OL sample was carried out according to AACC (1999). The moisture content was determined using gravimetric basis by oven drying of the oleosome sample at 105 °C (AACC 44–01.01); protein content was determined using Kjeldahl method to measure the free nitrogen content and converted to total protein with a conversion factor of 6.25 (AACC 46–30.01). The fat content of OLs was determined using Soxhlet method (AACC 30–25.01) whilst the ash content was determined upon incineration in a furnace at 550 °C for 12 h (AACC 08–16.01). The carbohydrates were calculated by subtraction *i.e.* 100-(moisture + ash + protein + fat). The composition was expressed on fresh weight basis of the extracted OL and shown in Fig. 1.

2.2.4. Sodium dodecyl sulphate polyacrylamide gel electrophoresis (SDS PAGE)

Protein composition of the OL cream after centrifugation at 25,000 rpm for 20 min and three times washing with MilliQ water was analysed using sodium dodecyl sulphate polyacrylamide gel electrophoresis (SDS-PAGE) using Invitrogen Novex 16% Tricine Protein Gels using Novex Tricine SDS Running Buffer (Fisher Scientific, Leicestershire, UK) according to the manufacturer's instructions. Novex Sharp Pre-Stained Protein Standard was used as the molecular mass standard and gels were stained using a Coomassie based stain (Invitrogen, SimplyBlue SafeStain). After destaining, gels were imaged using a ChemiDoc XRS + imager using Image Lab software (Bio-Rad, Hertfordshire, UK).

2.2.5. Confocal scanning laser microscopy (CLSM)

The microstructures of the OL sample were characterized before and after subjecting to tribological stress and also before and after storage for 3 weeks with or without addition of 200 mM NaCl or 50 mM $CaCl_2$ using a Zeiss LSM 880 inverted confocal microscope (Carl Zeiss MicroImaging

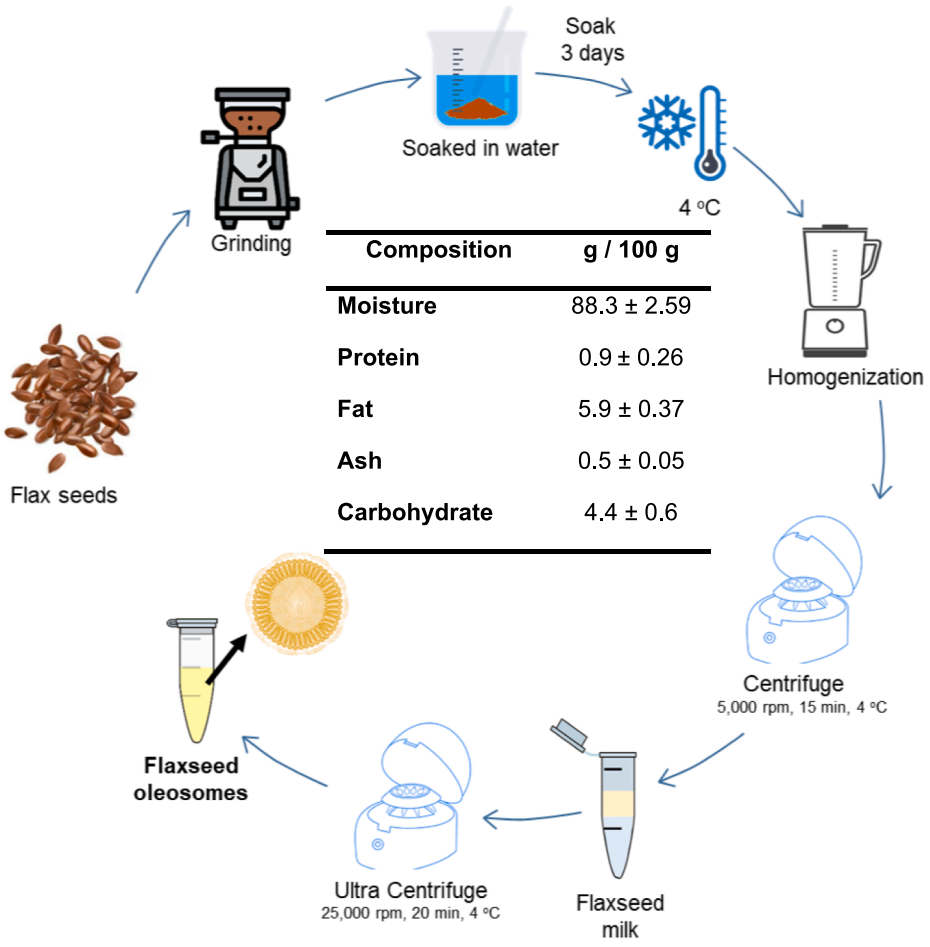

Composition	g / 100 g
Moisture	88.3 ± 2.59
Protein	0.9 ± 0.26
Fat	5.9 ± 0.37
Ash	0.5 ± 0.05
Carbohydrate	4.4 ± 0.6

Fig. 1. Schematic flow diagram for extraction of flaxseed oleosome (OL) sample with from flaxseeds with inset table showing the proximate composition of OL in fresh weight basis represented as means and standard error of means (SEMs) (n = 1 × 3).

GmbH, Jena, Germany). Approximately, 5 μL of Nile Red solution (0.1 % v/w in dimethyl sulfoxide) and Fast Green solution (1.0 %v/w in MilliQ water) were used to fluorescently stain the lipid (excited at 514 nm) and protein phases (excited at 633 nm) of the OL, respectively. The fluorescently labelled OL sample was placed on a concave confocal microscope slide, fixed with a glass coverslip, and imaged using an oil-immersion 63 × lens and pinhole diameter 1 Airy Unit to filter out most of the light scattering.

2.2.6. Cryogenic-scanning electron microscopy (cryo-SEM)

For cryo-SEM imaging of freshly extracted OL samples, previous method described by Shi, Chen, and Meng (2023) was employed with slight modifications. Cryo-SEM micrographs of OL were taken by the electron microscope (Tescan Amber X, Kohoutovice, Czech Republic). The OLs were snap-frozen in liquid nitrogen at − 180 °C for 30 s, and transferred immediately to the sample preparation chamber on the SEM. The frozen OLs were cleaved and then etched at − 90 °C for 4 min. Next, the samples were coated with 5 nm of platinum (Pt). Finally, the Pt-coated samples were transferred to the SEM for imaging at − 140 °C and imaged at an acceleration voltage of 2.0 kV (Quorum PP3010T system).

2.2.7. Droplet size measurements

The droplet size distributions of the OLs were determined using static light scattering at 25 °C using a Malvern MasterSizer 3000 (Malvern Instruments Ltd, Malvern, Worcestershire, UK). The mean droplet size distribution of the OLs samples at different pH (pH 1.0 3.0, 5.0 7.0 and reference pH of pH 5.4) and ionic strengths (50 mM NaCl, 200 mM NaCl, 5 mM $CaCl_2$, 5 mM $CaCl_2$, 200 mM NaCl + 50 mM $CaCl_2$) as a function of storage period for 9 weeks was reported along with their volume mean diameter, d_{43} (De Brouckere mean diameter) and the surface mean diameter, d_{32} (Sauter mean diameter). The relative refractive index, *i.e.* the ratio of oil (1.456) to that of the aqueous medium (1.33), was 1.095.

2.2.8. ζ-potential measurements

The electrophoretic mobility of the OL sample at various ionic strength and pH were measured using a Zetasizer (ZS Nano, Malvern Instruments Ltd, Malvern, UK). The diluted emulsion samples (0.05 wt% droplet concentration) were transferred into a folded capillary cells (Model DTS1070, Malvern Instruments Ltd., Worcestershire, UK) for measurement. The electrophoretic mobility was then converted to ζ-potential values using the classical Smoluchowski equation.

2.2.9. Rheology

Apparent viscosities of OL and flaxseed oil (FSO) were measured using a modular compact rheometer (MCR-302, Anton Paar, Austria). A cone- plate geometry system (CP50-1, angle 1°) was used and apparent viscosities were measured as a function of shear rate ranging from 0.01 to 1000 s^{-1} at 37 °C. The hysteresis was negligible for the tested samples. About 2.0 mL of the OL or FSO was placed onto the sample plate and sealed with the temperature hood to maintain the sample at specified temperature and prevent evaporation.

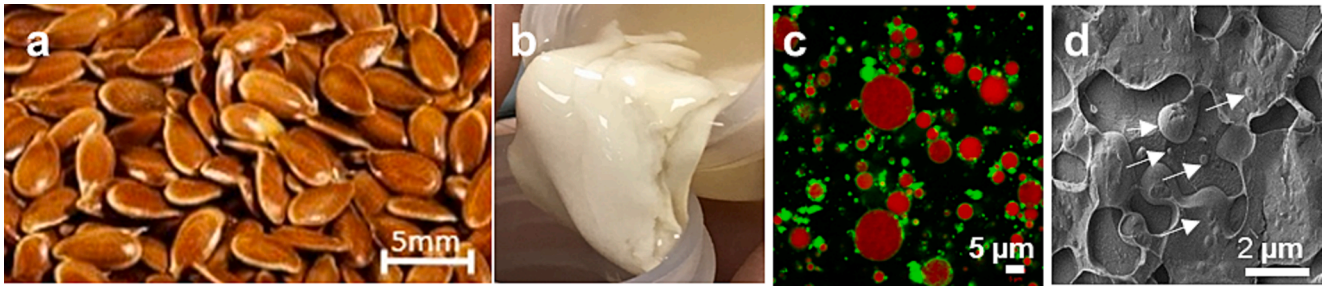

Fig. 2. Macroscopic image of flaxseed (a) and multiscale images of OL with macroscopic image (b), confocal laser scanning micrograph (c) and cryo-SEM image (d) with white arrows pointing the OL droplets.

2.2.10. Tribology

A Mini Traction Machine 2 (MTM2, PCS Instruments, London, UK) containing hydrophobic PDMS ball and disc as tribo-pairs was used to determine the tribological properties of the OL and FSO samples. A normal load of 2 N (Hertzian contact pressure of 343 kPa) and a slip-to-roll ratio (SRR) of 50% was used for all friction measurements. Friction coefficients (μ) were measured for all samples as a function of entrainment speed (U); the speeds ranged from 1 to 1000 mm s^{-1}. Analyses were carried out by fixing the temperature to 25 or 37 °C.

2.2.11. Statistical analysis

All the extractions and measurements were performed at least in triplicates ($n = 3 \times 3$) unless otherwise specified. The statistical analyses were conducted using one-way ANOVA followed by the Tukey's pairwise comparison with a 95% confidence interval using SPSS software (IBM, SPSS statistics, version 24).

3. Results and discussion

3.1. Composition and microstructure of flaxseed oleosome

The proximate composition of the extracted OL sample is shown in Fig. 1. The extracted OL contained nearly 1 w% protein, 6 wt% oil and 88.3 wt% water, the latter been higher than that of studies reporting the composition of oleosome derived from other oil seeds (Li, Wang, Hao, & Xu, 2022; Romero-Guzmán, 2020). While the high moisture ratio might be related to the extraction method, the oil: protein ratios of OL was in agreement with previous literature (Fig. 1) (Kapchie, Hauck, Wang, & Murphy, 2011; Nikiforidis, Matsakidou, & Kiosseoglou, 2014; Tontul & Sert, 2021). Generally, the ratio of oil to protein in emulsions, and hence in oleosomes, is crucial to govern the stability of the droplets. The relatively high carbohydrate content observed in the OL sample may be attributed to the presence of high mucilage content in flaxseeds (Chen et al., 2006). This additional carbohydrate component could potentially

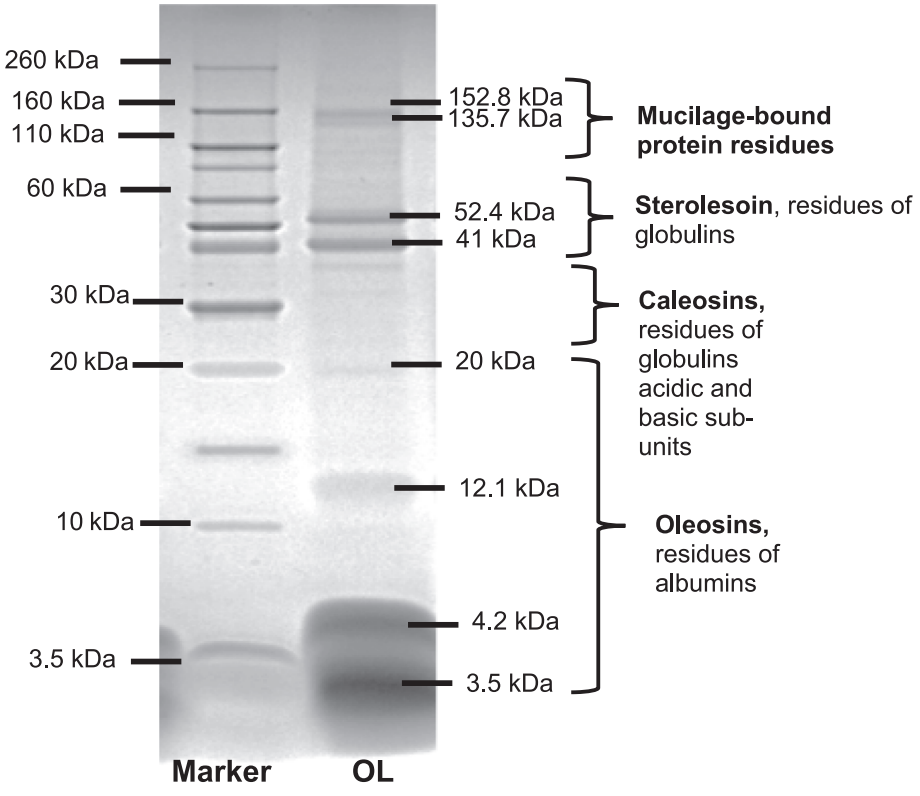

Fig. 3. SDS-PAGE of OL sample showing the protein units. Lane Marker represents the protein marker of 3.5–260 kDa molecular weight range.

Table 1
Mean droplet size (μm) and ζ-potential (mV) of oleosome (OL) samples as a function of storage period for P0 (immediately after preparation), P1 (3 weeks storage), P2 (9 weeks storage) and P3 (9 weeks) storage at 25 °C with/ without changing the pHs from pH 1.0–7.0 and ionic strengths (0–200 mM NaCl, 0–50 mM $CaCl_2$, 200 mM NaCl + 50 mM $CaCl_2$). Superscript letters and Greek alphabets (only within same measuring metrics *i.e.* d_{32} or d_{43}) within following mean values denote significant difference at $p < 0.05$ across column and row, respectively. Experiments have been performed three times on triplicates samples (n = 3 × 3).

	Mean ± Standard deviations d_{32} (μm)				Mean ± Standard deviations d_{43} (μm)				Mean ± Standard deviations ζ-potential (mV)
	P0	**P1**	**P2**	**P3**	**P0**	**P1**	**P2**	**P3**	**P0**
pH 1.0	2.15 ± 0.03 $^{a\alpha}$	3.99 ± 0.00 $^{b\beta}$	4.29 ± 0.01 $^{b\beta}$	4.94 ± 0.02 $^{b\gamma}$	9.26 ± 0.10 $^{b\alpha}$	15.66 ± 0.15 $^{c\beta}$	17.48 ± 0.15 $^{c\beta}$	19.66 ± 0.05 $^{d\gamma}$	+2.91 ± 0.79 ^{a}
pH 3.0	1.79 ± 0.01$^{a\alpha}$	2.73 ± 0.03 $^{a\alpha}$	2.69 ± 0.00 $^{a\alpha}$	2.81 ± 0.00 $^{a\alpha}$	6.34 ± 0.14 $^{a\alpha}$	11.75 ± 2.13 $^{b\beta}$	7.32 ± 0.08 $^{a\alpha\beta}$	8.03 ± 0.12 $^{a\alpha\beta}$	−0.28 ± 0.04 ^{a}
pH 5.0	1.8 ± 0.01 $^{a\alpha}$	3.23 ± 0.17 $^{ab\beta}$	3.12 ± 0.01 $^{a\beta}$	3.18 ± 0.01 $^{a\beta}$	4.87 ± 0.13 $^{a\alpha}$	16.55 ± 3.32 $^{c\gamma}$	10.42 ± 0.13 $^{b\gamma}$	11.56 ± 0.29 $^{b\gamma}$	−18.8 ± 0.98 ^{d}
pH 5.4[r]	1.65 ± 0.00 $^{a\alpha}$	2.69 ± 0.00 $^{a\alpha\beta}$	2.88 ± 0.1 $^{a\alpha\beta}$	3.04 ± 0.02 $^{a\beta}$	4.04 ± 0.05 $^{a\alpha}$	8.32 ± 0.23 $^{a\beta}$	11.12 ± 0.18 $^{b\beta\gamma}$	12.63 ± 0.39 $^{b\gamma}$	−23.3 ± 0.40 ^{e}
pH 7.0	2.16 ± 0.02 $^{a\alpha}$	3.08 ± 0.02 $^{a\beta}$	3.05 ± 0.01 $^{a\beta}$	4.26 ± 0.03 $^{b\gamma}$	11.50 ± 0.61 $^{c\alpha}$	10.60 ± 0.19 $^{b\alpha}$	12.24 ± 0.11 $^{b\alpha}$	20.86 ± 0.50 $^{de\beta}$	−41.0 ± 1.21 ^{f}
50 mM NaCl	1.72 ± 0.06 $^{a\alpha}$	2.66 ± 0.00 $^{a\alpha}$	2.96 ± 0.31 $^{a\beta}$	3.18 ± 0.08 $^{a\beta}$	5.66 ± 0.76 $^{a\alpha}$	7.97 ± 0.18 $^{ab\alpha}$	19.22 ± 1.63 $^{d\beta}$	22.47 ± 1.76$^{b\gamma}$	−11.1 ± 0.52 ^{c}
200 mM NaCl	1.82 ± 0.02 $^{a\alpha}$	2.64 ± 0.15 $^{a\beta}$	2.65 ± 0.00 $^{a\beta}$	2.70 ± 0.01 $^{a\beta}$	5.47 ± 0.00 $^{a\alpha}$	9.96 ± 0.54 $^{b\beta}$	7.99 ± 0.04 $^{a\alpha\beta}$	8.52 ± 0.22 $^{a\alpha\beta}$	−19.0 ± 0.62 ^{d}
5 mM $CaCl_2$	1.78 ± 0.04 $^{a\alpha}$	2.55 ± 0.01 $^{a\beta}$	2.76 ± 0.01 $^{a\beta}$	2.86 ± 0.03 $^{a\beta}$	6.31 ± 0.38 $^{a\alpha}$	5.93 ± 0.12 $^{a\alpha}$	8.68 ± 0.18 $^{a\beta}$	10.19 ± 0.42 $^{ab\gamma}$	−7.53 ± 0.68^{b}
50 mM $CaCl_2$	2.17 ± 0.12 $^{a\alpha}$	3.10 ± 0.02 $^{\beta}$	3.71 ± 0.04 $^{ab\beta}$	3.95 ± 0.10 $^{ab\beta}$	58.6 ± 12.56 $^{d\delta}$	13.28 ± 3.12 $^{bc\alpha}$	17.78 ± 1.27 $^{c\alpha\beta}$	21.97 ± 2.64 $^{c\gamma}$	−5.61 ± 0.25^{b}
200 mM NaCl + 50 mM $CaCl_2$	2.03 ± 0.05 $^{a\alpha}$	2.75 ± 0.02 $^{a\alpha\beta}$	3.09 ± 0.01 $^{a\alpha\beta}$	3.20 ± 0.02 $^{a\beta}$	8.79 ± 0.12 $^{ab\alpha}$	7.43 ± 0.28 $^{ab\alpha}$	12.00 ± 0.61 $^{b\beta}$	14.64 ± 0.72 $^{c\beta}$	−9.45 ± 1.44 ^{bc}

[r] Reference sample with unchanged pH (pH 5.4) and ionic strength *i.e.* without any added ions. All the ions are added with pH being maintained at pH 7.0.

contribute to the kinetic stability of the droplets, as will be discussed later.

The flaxseeds used in this study and the microstructures of the OL at various length scales are presented in Fig. 2. The OL freshly extracted from flaxseeds (Fig. 2**a**) without any pH or ionic adjustments exhibited a mayonnaise-like appearance (Fig. 2**b**), which is consistent with previous reports from (Romero-Guzmán, Köllmann, Zhang, Boom, & Nikiforidis, 2020a). To investigate the structure of the extracted flaxseed oleosomes, confocal microscopy (CLSM) was employed. As shown in Fig. 2**c,** OL were spherical droplets that appeared in various diameters from sub-micron sizes until a few μm, which was consistent with previous studies reporting oleosomes from other oilseed sources (Karefyllakis, Octaviana, van der Goot, & Nikiforidis, 2019). The green areas show presence of proteins as a monolayer or as aggregates surrounding the hydrophobic lipid core. The protein: oil ratio of 1: 6 w/w (Fig. 1) is generally sufficient to create a monolayer at the droplet surface, depending upon the interfacial properties of the protein coating the droplets. Nevertheless, in some instances, the proteins are forming bridges between the OL droplets showing flocs of few neighbouring droplets together (Fig. 2**c**). Going further down in length scales, droplets in cryo-SEM (Fig. 2**d**) can be observed of the same size range as seen in Fig. 2**c** with slightly elevated parts defining the borders of these droplets representing the protein domains.

Fig. 3 shows the SDS-PAGE profile of OL cream layer to understand which proteins where dominating the surface of these OL droplets. The electrogram shows eight distinguishable bands between 3.5 k_D and 152.8 kDa with further bands that were fainter. All of these proteins in the form of aggregates were present at the surface to coat the hydrophobic lipid core as observed in Fig. 2**c**. Of these eight bands, four bands corresponding to 3.5 kDa, 4.2 kDa, 41 kDa and 52.4 kDa were observed to be prominent. Chung, Lei, and Li-Chan (2005) reported that they detected eleven (three dominant bands (20, 23 and 31 kDa)) and fifteen (three dominant bands (20, 23 and 31 kDa)) bands from the proteins extracted from hulled and defatted flaxseed, according to the reducing and non-reducing SDS-PAGE conditions, respectively. It is thought that some differences observed in the protein fraction of OL versus previous studies are due to the applied oleosome extraction conditions, seed type and analysis conditions. In the study of Lan, Ohm, Chen, and Rao (2020), the molecular weight profiles of two flaxseed globulins and albumins, with molecular weights ranging from 10 to 52 kDa were observed. Similarly, Tirgar, Silcock, Carne, and Birch (2017) reported that the main fraction of three different flaxseed protein concentrates comprised globulin and albumin. However, the number and proportions of protein units was observed to vary depending on the extraction conditions. Based on previous researches of flaxseed oleosomes and oil bodies from other seed sources, the protein bands in OL < 20 kDa might be attributed to olesoins, 20–40 kDa were most likely caleosins, whilst steroleosins were most likely the > 40 to < 60 kDa protein bands (Fig. 3) (Chung et al., 2005; Lan et al., 2020; Nwachukwu & Aluko, 2018; Tirgar et al., 2017). Nevertheless, residues of flaxseed albumins and globulins even after subsequent centrifugation and aqueous extractions steps cannot be underestimated at the surface of OL droplets. Unlike most previous studies, OL also included two prominent high molecular weight bands of 137.5 kDa and 152.8 kDa, such protein bands might be associated with the mucilages, which were also extracted together with the OL. The relative band intensity associated with medium (40–50 kDa) and low (3.5–12 kDa) molecular weight protein bands in OL was significantly higher when comparing with those in the high molecular weight polypeptides (>100 kDa) (Fig. 3). This suggests that OL contained a larger proportion of low to medium molecular weight fractions whilst the demucilaging diminished even if not completely removed the larger polypeptides during the aqueous extraction and centrifugation process. In summary, these higher molecular weight proteins alongside higher concentrations of the lower molecular weight oleosins, caleosins, albumins and globulins provided steric stabilization to the OLs (6: 1 w/w ratio of oil to protein) (Fig. 1) against coalescence as observed in the

confocal micrographs (Fig. 2**b**).

3.2. Responsiveness of flaxseed oleosomes to pH

To understand whether electrostatic interaction was key to the kinetic stability of OLs, electrokinetic potentials were recorded as a function of pH. OLs were negatively-charged at neutral pH (Table 1). Even at their natural pH of extraction (pH 5.4), they had significant negative surface charge (–23 mV), which highlights the importance of charge-mediated repulsive being sufficient to retain the dispersity of OLs as shown in Fig. 2. Unlike other oil bodies such as those derived from soybean (Qi et al., 2017), sunflower and rapeseed (Romero-Guzmán et al., 2020a), OLs possessed high negative charge (-41 mV) at neutral pH highlighting the benefit of these flaxseed oleosomes in food development. One can expect both low molecular weight proteins as well as mucilages contributing to this negative surface charge at OL surface as flaxseed mucilages are also anionic in nature (Chen et al., 2006).

The stability of OLs against flocculation and coalescence is largely dependent on the repulsive forces between the proteins adsorbed onto the OL surface, which might alter based on pH change. Particularly, the

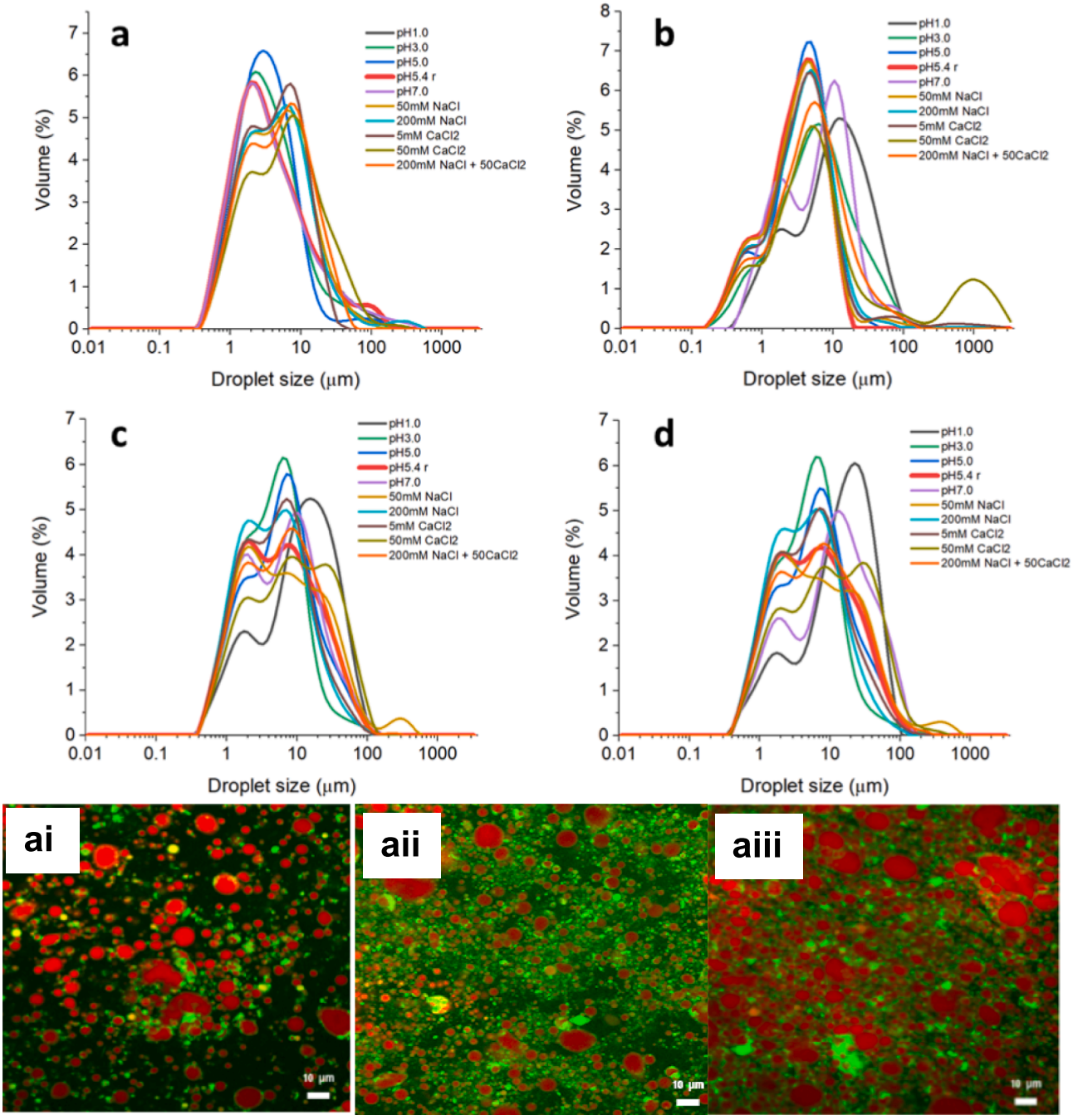

Fig. 4. Mean droplet size distribution of OL at different conditions (pH (pH 1.0–7.0) and ionic strengths (0–200 mM NaCl, 0–50 mM $CaCl_2$) stored for different time periods: a, 0 week *i.e.* week of preparation; b, 3 weeks of storage; c, 6.weeks of storage and d, 9 weeks of storage. Confocal images of corresponding emulsions without ions (ai) and with addition of 200 mM NaCl (aii) or with 50 mM $CaCl_2$ (aiii) are shown with protein aggregates stained fluorescently green using Fast green whilst fat droplets are stained fluorescently red using Nile Red.

ζ-potential values gradually changed from negative to positive as the pH decreased from 7.0 to 1.0 ($p < 0.05$) with net charge values decreasing significantly at low pH value. For example, the ζ-potentials was closer to zero at pH 3.0, owing to amino side groups ($–NH_3^+$) being equivalent to the carboxylic acid groups ($–COO^-$). This suggests the isoelectric point of the proteins stabilizing the OL droplets were closer to pH 3.0 (Table 1). Interestingly, this is far from the *pI* generally reported for purified oleosins (pH 4.5–5.5), highlighting again the importance of multiple protein subunits such as caleosins, sterolesosins as well as residues of non-membrane proteins (*e.g.* albumins, globulins and mucilage-bound proteins) (Fig. 3) contributing to the surface charge and overall kinetic stability of the OLs.

Looking at the droplet size distributions of OL immediately after preparation (Fig. 4**a**), pH did not affect the peak breadth ranging in size from 0.5 to 50 μm with a limited impact on d_{32} values ($p > 0.05$) (Table 1). Similar results were reported previously for oleosomes derived from other plant sources with pH having minimal effect on oleosome stability when the pH is far from the *pI* (Qi et al., 2017). However, due to charge-mediated aggregation, there was some variation in larger-sized droplet population and consequently d_{43} was higher at pH 1.0 and pH 7.0 ($p < 0.05$) as compared to the natural pH of extraction (Table 1).

3.3. Responsiveness of flaxseed oleosomes to mono and divalent ions

Generally, oil bodies may flocculate or coalesce when the ionic strength exceeds a particular level (Romero-Guzmán et al., 2020b). This is because the ions screen the charges and therefore the net repulsive electrostatic forces between the oleosome droplets may not be sufficient to overcome the hydrophobic or van der Waal's attractive forces. To understand this, OLs were subjected to both mono (0–200 mM NaCl) and divalent cations (0–50 mM $CaCl_2$) at pH 7.0. Presence of both mono and divalent cations irrespective of their concentration significantly reduced the net surface charge versus OLs without any added ions ($p < 0.05$) with most marked reduction in absolute magnitude of ζ-potential happening in presence of Ca^{2+} ions (-5.6 mV) (Table 1). This was also in line with a significant shift in the droplet size distribution with double-humped peak shifting to > 10 μm-sized droplets particularly in presence of 50 mM $CaCl_2$ (Fig. 1**a**) and consequently the size of the droplets increased by nearly 15× ($d_{43} = 59$ μm) ($p < 0.05$) (Table 1). Such salt induced aggregation has also been previously observed in rapeseed and nut-based oleosomes (Romero-Guzmán et al., 2020b; Zhou, Chen, Hao, Du, & Liu, 2019) having different *pI* versus OLs derived from flaxseed in the currents study. Looking at the confocal micrographs (Fig. 4**ai-iii**), it is clear that presence of monovalent ions (200 mM NaCl) had much more green fluorescence as compared to the ones without ions highlighting the occurrence of protein–protein aggregation in OLs. In addition, some non-spherical coalesced OL droplets were indeed evident in presence of NaCl, which might be associated with NaCl-induced charge screening effects (Table 1) and compression of electrostatic double layer reducing the net repulsive forces between the droplets. The droplet coalescence in OLs were prominent in presence of Ca^{2+} ions showing large pool of uncoated oil droplets in line with the droplets size data (Table 1). Such dramatic increase in presence Ca^{2+} might be attributed to the calcium binding to caleosins (Næsted et al., 2000), the flaxseed mucilages containing calcium-binding galacturonic acid (Chen et al., 2006). These compounds can be compared to pectin, which might have brought the OL droplets in close vicinity, leading to droplet flocculation and coalescence. To our knowledge, this is the first systematic study that reports the effect of pH and ions highlighting the important effect of Ca^{2+} ions on destabilization of oleosomes derived from flaxseeds, which might have implications when OLs are employed in food product development.

3.4. Storage stability of flaxseed oleosomes

Understanding microstructural stability of oleosomes in absence or presence of environmental stresses is crucial for long-term preservation of the samples as well as subsequent utilization in food processing (Abdullah, Weiss, & Zhang, 2020). Despite the importance, microstructural stability of osmoses under storage has seldom been reported in literature with no published report on OLs derived from flaxseeds. Looking at OLs at pH 7.0 in absence of ions, the droplet size distributions showed minimal variations, particularly as a function of storage (Fig. 4**a-d**). The d_{32} remaining fairly constant throughout, while the d_{43} exhibited a slight but non-significant increase to 12.2 μm until 6 weeks and significant increase to 20 μm only after 9 weeks of storage ($p > 0.05$) (Table 1). The latter showed no signs of coalescence (confocal data not shown). Even when subjected to monovalent ions and/or pH alterations (Fig. 4 **b-d**), the OLs were relatively stable with d_{43} values ranging from 6 to 22 μm (Table 1) during 9 weeks of storage period. One should take the sizing data in presence of Ca^{2+} ions with some caution, which in fact reduced in size with storage (Table 1). This is most likely related to the coalesced droplets (see Fig. 4**aiii**) being moved to the top and were not effectively captured during the light scattering experiments Fig. 4**b-d**).

To sum it up, OLs showed excellent storage stability with marked destabilization only in presence of divalent ions. Often hydrocolloids with high molecular weights such as pectin and alginates are used to provide steric stability to oleosomes against flocculation and coalescence (Mert & Vilgis, 2021; Zhang et al., 2019) but this was not required in case of OLs. The OLs in this study had high kinetic stability unlike most reported oleosomes– thanks to the residues of inherently present flaxseed gums at the interface of OL droplets, which might have offered additional steric stability.

3.5. Viscosity and lubricity of flaxseed oleosomes

Considering the OLs had varying degree of coalescence in presence of ions, we performed the rheological and tribological experiments using only the stable OLs without any added salts at pH 7.0 to clearly understand the destabilization effects (if any) of purely applied shear. Firstly, we measured flaxseed oil (FSO) as a control, which shows typical Newtonian behaviour with almost constant apparent viscosity of about ~ 25 to 30 mPa.s over the entire range of the applied shear rates (Fig. 5**a**). Findings regarding the FSO sample in this study are similar to those reported in previous studies reporting flaxseed oil obtained from various flax plants (Punia, Sandhu, Dhull, Kaur, & Siroha, 2020; Zhang, Wang, Li, Li, & Özkan, 2011).

The OLs on the other hand demonstrated a significant shear thinning behaviour (Fig. 5**a**) with viscosity decaying by two orders of magnitude to ~ 20 mPa.s as a function of shear rate studied. Despite having only 6 wt% oil (Fig. 1), the system still possessed significant viscosity resembling those of sunflower oleosomes containing nearly 40 wt% oil at corresponding shear rates (White, Fisk, Mitchell, Wolf, Hill, & Gray, 2008). Such high viscosity and sharp shear thinning character of FSO might be attributed to the weak depletion-type droplet flocculation occurring in OLs at pH 7.0. Even at 50 s^{-1} shear rate, which is often considered to be in line with shear rates occurring in mouth conditions (Ong, Steele, & Duizer, 2018), the viscosity was 2.5 × higher than that of flaxseed oil (FSO), suggesting that OL retained the emulsion-like structure despite subjected to the shear rates (Fig. 5**a**). However, above 450 s^{-1}, the OLs behaved like FSO, highlighting that the emulsions were disrupted by the shear into an oil film. Although such high shear rates might be less relevant in the rheological limit, they can have a significant effect on the tribological performance of OL, especially in narrow gaps where shear rates are generally higher than 1000 s^{-1} (Sarkar, Andablo-Reyes, Bryant, Dowson, & Neville, 2019). Additionally, behaviour in such tribological limits might translate into interesting mouthfeel consequences, such as smoothness and creaminess (Sarkar & Krop, 2019).

Fig. 5**b-c** show the frictional performance of OL and FSO with water as a control in soft tribological contacts at different temperature (25 and 37 °C) conditions. As one might expect, water had high friction

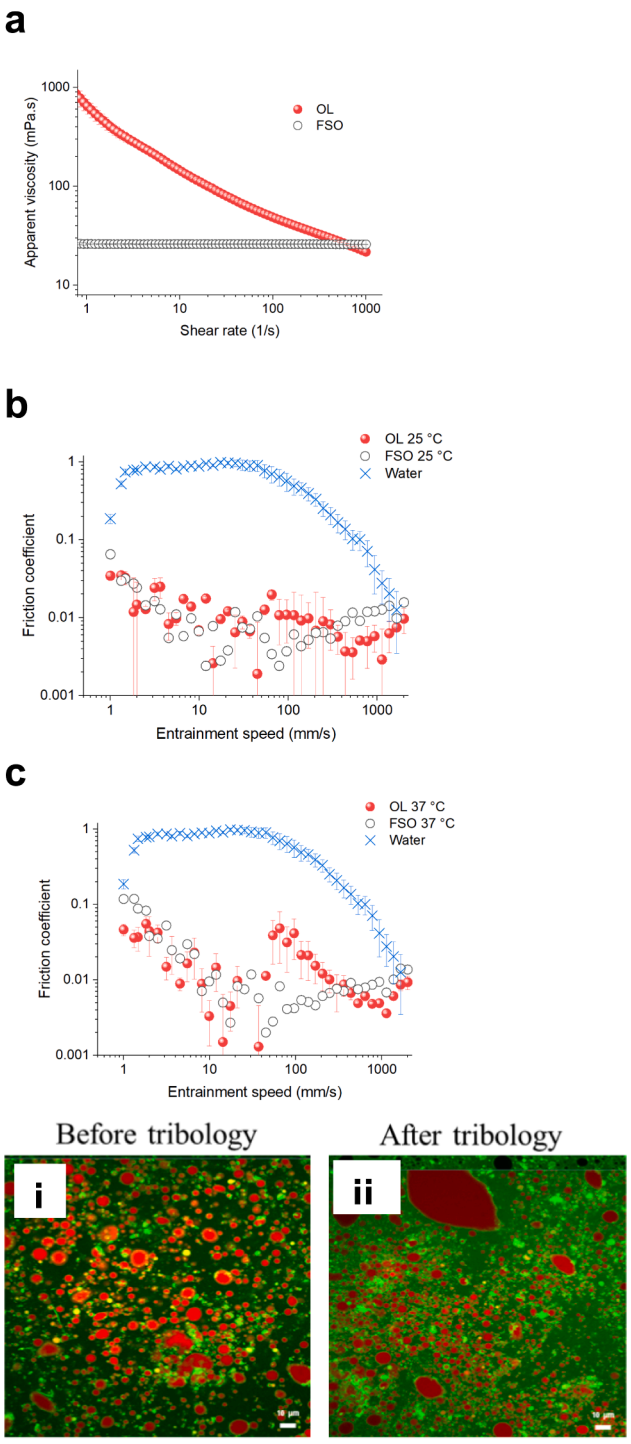

Fig. 5. Mean apparent viscosity (a) of OLS and flaxseed oil (FSO) as a function of shear rate, mean friction coefficients as a function of entrainment speeds at (b) 25 °C and (c) 37 °C. Confocal images before (i) and after exposure to tribological stress (ii) are also shown in c. Error bars represent standard deviation of three measurements on triplicate samples (n = 3 × 3).

coefficients, which might be attributed to the inability of water to form a lubricating film in between PDMS-based hydrophobic contact surfaces. Interestingly, the tribological behaviour of FSO (Fig. 5**b-c**), irrespective of temperature, was similar to those of other vegetable oils containing unsaturated fatty acids (Torres, Andablo-Reyes, Murray, & Sarkar, 2018) with friction coefficients < 0.05 maintained in the mixed regime. To date, limited tribological studies have been performed on oleosomes. For example, the friction of soybean-based oil bodies in the mixed regime has been found to be higher than that of the corresponding soybean oil (Yang et al., 2020). Strikingly, irrespective of the speeds, the OL in this study resembled the frictional profile of FSO in the mixed regime but slightly differed in the onset of elastohydrodynamic regime. The electrohydrodynamic regime for OLs occurred at a 5 × lower speed, while for FSO, it was at 20 × lower speed (~100 mm s^{-1} and 50 mm s^{-1} at 25 °C and 37 °C, respectively) as compared to those in OLs. This suggest that OL has somehow destabilized in the tribological contact and formed a coalesced film. This was further evidenced by confocal images pre- and post-tribology (Fig. 5**ci** and **ii**) of OLs, which show a high degree of coalescence and uncoated smaller OLs, which might have resulted from droplet breakup during triboshearing versus the pre-tribology samples. Overall, this suggests that the OLs extracted from flaxseed had a limited resistance to coalescence in tribological conditions, which might be in fact beneficial in providing desired mouthfeel if used for designing plant-based foods.

4. Conclusions

In this study, oleosome samples were extracted from flaxseed using a facile, green, aqueous extraction method under low temperature and pH close to natural conditions, with no addition of organic solvents. The oleosomes were stabilized by a range of lower to higher molecular weight proteins including ones hypothesised to be associated with mucilages. Using a combination of microscopy across length scales, electrophoresis and light scattering, we confirmed, for the first time, the kinetic stability of these oleosomes stabilized by proteins of 3.5–152.8 kDa over 6 weeks storage. This stability can be largely attributed to electrostatic repulsive forces generated by the flaxseed proteins, whilst steric stabilization offered by larger glycans associated with mucilage. Varying degree of kinetic stability was evidenced in presence of ions and pH conditions with most dramatic effects of coalescence observed in presence of Ca^{2+} ions due to ion binding to oleosome-associated surface proteins. Strikingly, the oleosomes show a high shear thinning behaviour despite containing just 6 wt% oil. Of more importance, the unprecedented tribological properties of flaxseed oleosome was similar to those of flaxseed oil highlighting the shear-induced coalescence of these oleosomes. In summary, this study sets the scene for using flaxseed oleososme as a potential natural emulsion for designing plant-based products without added emulsifiers to offer the desired rheological as well as tribological benefits. Future studies are underway exploring the sensorial and gastrointestinal digestion of these naturally derived emulsions.

CRediT authorship contribution statement

Hasan H. Kara: Writing – original draft, Methodology, Validation, Formal analysis, Investigation, Data curation, Writing – review & editing, Visualization, Funding acquisition. **Andrea Araiza-Calahorra:** Methodology, Formal analysis, Investigation, Data curation, Visualization, Writing – review & editing. **Neil M. Rigby:** Methodology, Formal analysis, Investigation, Data curation. **Anwesha Sarkar:** Methodology, Conceptualization, Data curation, Writing – review & editing, Visualization, Supervision.

Declaration of Competing Interest

The authors declare that they have no known competing financial interests or personal relationships that could have appeared to influence the work reported in this paper.

Data availability

Data will be made available on request.

Acknowledgements

Funding from the European Research Council (ERC) under the European Union's Horizon 2020 research and innovation programme (grant agreement n° 757993) is acknowledged. Author Dr. Hasan H. Kara acknowledges funding from The Scientific and Technological Research Council of Türkiye (TUBITAK) under 2219-International Postdoctoral Research Fellowship Program for his visiting research at the University of Leeds, UK.

References

AACC. (1999). Approved methods of analysis (11th Ed.). Retrieved from: http://methods.aaccnet.org/toc.aspx Accessed.

Abdullah, Weiss, J., & Zhang, H. (2020). Recent advances in the composition, extraction and food applications of plant-derived oleosomes. *Trends in Food Science & Technology, 106*, 322–332. https://doi.org/10.1016/j.tifs.2020.10.029

Acevedo-Fani, A., Dave, A., & Singh, H. (2020). Nature-assembled structures for delivery of bioactive compounds and their potential in functional foods. *Frontiers in Chemistry, 8*. https://doi.org/10.3389/fchem.2020.564021

Chang, M.-T., Tsai, T.-R., Lee, C.-Y., Wei, Y.-S., Chen, Y.-J., Chen, C.-R., & Tzen, J. T. (2013). Elevating bioavailability of curcumin via encapsulation with a novel formulation of artificial oil bodies. *Journal of Agricultural and Food Chemistry, 61*(40), 9666–9671.

Chen, H.-H., Xu, S.-Y., & Wang, Z. (2006). Gelation properties of flaxseed gum. *Journal of Food Engineering, 77*(2), 295–303. https://doi.org/10.1016/j.jfoodeng.2005.06.033

Chen, Y., & Ono, T. (2010). Simple extraction method of non-allergenic intact soybean oil bodies that are thermally stable in an aqueous medium. *Journal of Agricultural and Food Chemistry, 58*(12), 7402–7407.

Chung, M. W. Y., Lei, B., & Li-Chan, E. C. Y. (2005). Isolation and structural characterization of the major protein fraction from NorMan flaxseed (Linum usitatissimum L.). *Food Chemistry, 90*(1), 271–279. https://doi.org/10.1016/j.foodchem.2003.07.038

De Chirico, S., di Bari, V., Foster, T., & Gray, D. (2018). Enhancing the recovery of oilseed rape seed oil bodies (oleosomes) using bicarbonate-based soaking and grinding media. *Food Chemistry, 241*, 419–426.

Kajla, P., Sharma, A., & Sood, D. R. (2015). Flaxseed—a potential functional food source. *Journal of Food Science and Technology, 52*, 1857–1871.

Kapchie, V. N., Hauck, C. C., Wang, H., & Murphy, P. A. (2011). Process improvement for semipurified oleosomes on a pilot-plant scale. *Journal of Food Science, 76*(6), C853–C860.

Karefyllakis, D., Octaviana, H., van der Goot, A. J., & Nikiforidis, C. V. (2019). The emulsifying performance of mildly derived mixtures from sunflower seeds. *Food Hydrocolloids, 88*, 75–85. https://doi.org/10.1016/j.foodhyd.2018.09.037

Lan, Y., Ohm, J.-B., Chen, B., & Rao, J. (2020). Physicochemical properties and aroma profiles of flaxseed proteins extracted from whole flaxseed and flaxseed meal. *Food Hydrocolloids, 104*, Article 105731. https://doi.org/10.1016/j.foodhyd.2020.105731

Li, X., Wang, Q., Hao, J., & Xu, D. (2022). Stability, Structure, Rheological Properties, and Tribology of Flaxseed Gum Filled with Rice Bran Oil Bodies. *Foods, 11*(19), 3110.

Mert, B., & Vilgis, T. A. (2021). Hydrocolloid coated oleosomes for development of oleogels. *Food Hydrocolloids, 119*, Article 106832. https://doi.org/10.1016/j.foodhyd.2021.106832

Næsted, H., Frandsen, G. I., Jauh, G.-Y., Hernandez-Pinzon, I., Nielsen, H. B., Murphy, D. J., … Mundy, J. (2000). Caleosins: Ca2+-binding proteins associated with lipid bodies. *Plant Molecular Biology, 44*(4), 463–476. https://doi.org/10.1023/A:1026564411918

Nikiforidis, C. V. (2019). Structure and functions of oleosomes (oil bodies). *Advances in Colloid and Interface Science, 274*, Article 102039. https://doi.org/10.1016/j.cis.2019.102039

Nikiforidis, C. V., & Kiosseoglou, V. (2011). Competitive displacement of oil body surface proteins by Tween 80 – Effect on physical stability. *Food Hydrocolloids, 25*(5), 1063–1068. https://doi.org/10.1016/j.foodhyd.2010.10.002

Nikiforidis, C. V., Kiosseoglou, V., & Scholten, E. (2013). Oil bodies: An insight on their microstructure — maize germ vs sunflower seed. *Food Research International, 52*(1), 136–141. https://doi.org/10.1016/j.foodres.2013.02.052

Nikiforidis, C. V., Matsakidou, A., & Kiosseoglou, V. (2014). Composition, properties and potential food applications of natural emulsions and cream materials based on oil bodies. *RSC Advances, 4*(48), 25067–25078.

Nwachukwu, I. D., & Aluko, R. E. (2018). Physicochemical and emulsification properties of flaxseed (Linum usitatissimum) albumin and globulin fractions. *Food Chemistry, 255*, 216–225. https://doi.org/10.1016/j.foodchem.2018.02.068

Ong, J. J., Steele, C. M., & Duizer, L. M. (2018). Challenges to assumptions regarding oral shear rate during oral processing and swallowing based on sensory testing with thickened liquids. *Food Hydrocolloids, 84*, 173–180. https://doi.org/10.1016/j.foodhyd.2018.05.043

Oomah, B. D. (2001). Flaxseed as a functional food source. *Journal of the Science of Food and Agriculture, 81*(9), 889–894.

Payne, G., Lad, M., Foster, T., Khosla, A., & Gray, D. (2014). Composition and properties of the surface of oil bodies recovered from Echium plantagineum. *Colloids and Surfaces B: Biointerfaces, 116*, 88–92.

Punia, S., Sandhu, K. S., Dhull, S. B., Kaur, M., & Siroha, A. K. (2020). Kinetic, rheological and thermal studies of flaxseed (Linum usitatissiumum L.) oil and its utilization. *Journal of Food Science and Technology, 57*(11), 4014–4021. https://doi.org/10.1007/s13197-020-04434-1

Qi, B., Ding, J., Wang, Z., Li, Y., Ma, C., Chen, F., … Jiang, L. (2017). Deciphering the characteristics of soybean oleosome-associated protein in maintaining the stability of oleosomes as affected by pH. *Food Research International, 100*, 551–557. https://doi.org/10.1016/j.foodres.2017.07.053

Romero-Guzmán, M. J. (2020). Designing a sustainable oleosome aqueous extraction: A new way to make emulsion-based foods. *Biobased Chemistry and Technology, Food Process Engineering*. Wageningen, Netherlands: Wageningen University and Research.

Romero-Guzmán, M. J., Köllmann, N., Zhang, L., Boom, R. M., & Nikiforidis, C. V. (2020). Controlled oleosome extraction to produce a plant-based mayonnaise-like emulsion using solely rapeseed seeds. *LWT, 123*, Article 109120. https://doi.org/10.1016/j.lwt.2020.109120

Romero-Guzmán, M. J., Petris, V., De Chirico, S., di Bari, V., Gray, D., Boom, R. M., & Nikiforidis, C. V. (2020). The effect of monovalent (Na+, K+) and divalent (Ca2+, Mg2+) cations on rapeseed oleosome (oil body) extraction and stability at pH 7. *Food Chemistry, 306*, Article 125578. https://doi.org/10.1016/j.foodchem.2019.125578

Sarkar, A., Andablo-Reyes, E., Bryant, M., Dowson, D., & Neville, A. (2019). Lubrication of soft oral surfaces. *Current Opinion in Colloid & Interface Science, 39*, 61–75. https://doi.org/10.1016/j.cocis.2019.01.008

Sarkar, A., & Krop, E. M. (2019). Marrying oral tribology to sensory perception: A systematic review. *Current Opinion in Food Science, 27*, 64–73. https://doi.org/10.1016/j.cofs.2019.05.007

Shi, Z., Chen, Z., & Meng, Z. (2023). Study on oil body emulsion gels stabilized by composited polysaccharides through microgel particles compaction and natural gelation. *Food Hydrocolloids, 135*, Article 108146.

Tirgar, M., Silcock, P., Carne, A., & Birch, E. J. (2017). Effect of extraction method on functional properties of flaxseed protein concentrates. *Food Chemistry, 215*, 417–424. https://doi.org/10.1016/j.foodchem.2016.08.002

Tontul, I., & Sert, D. (2021). Extraction and purification of oil bodies from pomegranate seeds. *Journal of Food Processing and Preservation, 45*(8), e15053.

Torres, O., Andablo-Reyes, E., Murray, B. S., & Sarkar, A. (2018). Emulsion microgel particles as high-performance bio-lubricants. *ACS Applied Materials & Interfaces, 10*(32), 26893–26905. https://doi.org/10.1021/acsami.8b07883

White, D. A., Fisk, I. D., Mitchell, J. R., Wolf, B., Hill, S. E., & Gray, D. A. (2008). Sunflower-seed oil body emulsions: Rheology and stability assessment of a natural emulsion. *Food Hydrocolloids, 22*(7), 1224–1232. https://doi.org/10.1016/j.foodhyd.2007.07.004

Wu, N., Yang, X., Zheng, E., Wang, L., Guo, J., Zhang, J., & Huang, X. (2012). Analysis of stability and rheology of soybean oil body emulsions. *Transactions of the Chinese Society of Agricultural Engineering, 28*(1), 369–374.

Yang, N., Feng, Y., Su, C., Wang, Q., Zhang, Y., Wei, Y., … Fang, Y. (2020). Structure and tribology of κ-carrageenan gels filled with natural oil bodies. *Food Hydrocolloids, 107*, Article 105945.

Zhang, Y., Yang, N., Xu, Y., Wang, Q., Huang, P., Nishinari, K., & Fang, Y. (2019). Improving the stability of oil body emulsions from diverse plant seeds using sodium alginate. *Molecules, 24*(21). https://doi.org/10.3390/molecules24213856

Zhang, Z.-S., Wang, L.-J., Li, D., Li, S.-J., & Özkan, N. (2011). Characteristics of Flaxseed Oil from Two Different Flax Plants. *International Journal of Food Properties, 14*(6), 1286–1296. https://doi.org/10.1080/10942911003650296

Zhou, L.-Z., Chen, F.-S., Hao, L.-H., Du, Y., & Liu, C. (2019). Peanut oil body composition and stability. *Journal of Food Science, 84*(10), 2812–2819. https://doi.org/10.1111/1750-3841.14801